ELSEVIER

Probabilistic Engineering Mechanics 20 (2005) 215–228

PROBABILISTIC ENGINEERING MECHANICS

www.elsevier.com/locate/probengmech

A translation model for non-stationary, non-Gaussian random processes

F.J. Ferrante*, S.R. Arwade, L.L. Graham-Brady

Department of Civil Engineering, The Johns Hopkins University, 202 Latrobe Hall, 3400 N. Charles Street, Baltimore, MD 21218 2686, USA

Available online 20 July 2005

Abstract

A model for simulation of non-stationary, non-Gaussian processes based on non-linear translation of Gaussian random vectors is presented. This method is a generalization of traditional translation processes that includes the capability of simulating samples with spatially or temporally varying marginal probability density functions. A formal development of the properties of the resulting process includes joint probability density function, correlation distortion and lower and upper bounds that depend on the target marginal distributions. Examples indicate the possibility of exactly matching a wide range of marginal pdfs and second order moments through a simple interpolating algorithm. Furthermore, the application of the method in simulating statistically inhomogeneous random media is investigated, using the specific case of binary translation with stationary and non-stationary target correlations.

Keywords: Stochastic simulation; Translation processes; Non-Gaussian processes; Non-stationary processes; Inhomogeneous materials; Random media; Functionally graded materials

1. Introduction

Modeling of uncertainty analysis in engineering problems via probabilistic simulation (i.e. Monte Carlo) has achieved considerable development in current probabilistic mechanics research. With the increase in available computational power, techniques for synthesis and estimation of stochastic processes have been able to include more complex characteristics such as multi-dimensionality, non-Gaussianity and non-stationarity.

Modeling of non-stationary processes has remained one of the greatest challenges in simulation. Analysis of environmental loads (such as wind pressure or seismic forces) pointed to the need for accurate representation of the time-dependent probabilistic content of phenomena. Early work on the subject by Priestley [1] led to the development of processes with evolutionary spectra, where a modulating function was used in order to characterize how the power spectrum of such records changed with respect to time. This was followed by the continuous development of non-stationary Gaussian simulation for specific applications using a wide range of techniques (i.e. [2–5] and [6]).

Equally important is the ability to extend simulation for cases in which Gaussian representation cannot characterize the random process with sufficient accuracy. To this end, methods based on spectral representation ([7–9]), translation processes [10] and polynomial expansion [11] have been developed.

Most of the work on non-Gaussian, non-stationary processes has been based on a homogeneous pdf (i.e. pdf at all points in time is the same), with a temporally varying non-stationary spectral density function. Less work is available for samples with spatially or temporally varying marginal pdfs. Some examples are [12], which considered mixtures of marginal distributions obtained through translation processes; [13], that presented a model to obtain samples with varying marginal pdfs at specific points using translation; [14], which used polynomial chaos expansion and [15], with a Karhunen-Loeve based iterative scheme.

This paper provides the theory to extend the translation technique with varying marginal pdfs for efficient simulation of non-Gaussian, non-stationary processes based on a continuously varying pdf, initially used in [16]. These processes are non-stationary in the sense that both the covariance used and the pdf may be temporally dependent. The approach does not require iteration in order to match target marginal pdfs and/or correlation function and, therefore, can be easily implemented for fast and efficient

* Tel.: +1 410 516 6144; fax: +1 410 516 7473.
E-mail address: fferrante@jhu.edu (F.J. Ferrante).

0266-8920/$ - see front matter © 2005 Elsevier Ltd. All rights reserved.
doi:10.1016/j.probengmech.2005.05.003

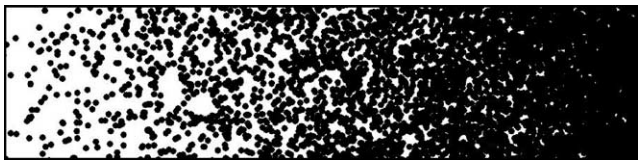

Fig. 1. Sketch of a functionally graded material with two phases (black and white), exhibiting a linear gradation from left to right.

simulation. Examples are used to demonstrate the applicability of the approach to vector processes.

Finally, the simulation of statistically inhomogeneous two-phase random media through binary representation is also considered as an application. An example of such media are functionally graded materials (see Fig. 1) in which the microstructure is intentionally changed with location. Extensive work has been done on homogeneous random media simulation (as in [17–20]). However, there are few examples of such simulations cases where the statistics on the material properties depend on the absolute position along the composite ([21–23]). Using the method developed here, samples of inhomogeneous binary processes with specific correlation functions are obtained.

2. Non-stationary translation processes

In this section, the new theoretical developments to non-stationary translation processes will be developed. Let $Z(t)$ be a non-stationary scalar valued random process with marginal cumulative distribution function $F(z, t)$ and marginal probability density function $f(z, t)$. If $F(z, t) = F(z, s)$, $\forall t,s$, and if certain constraints on the second moment properties are met, then the process can be modeled as a standard translation process [10]. If $F(z, t) \neq F(z, s)$ for any pair of time instants (t, s), then the process can be modeled, subject to a set of constraints which will be developed herein, as a non-stationary translation process

$$Z(t) = g(Y(t), t) = F_t^{-1} \circ \Phi(Y(t)) \tag{1}$$

where $F_t^{-1}(\cdot)$ is the inverse of $F(z, t)$, $\Phi(\cdot)$ is the standard Gaussian cdf and $Y(t)$ is a Gaussian random process. The process $Y(t)$ is stationary with respect to its marginal distribution and has mean zero and unit variance. The process $Y(t)$ may, however, have second moment properties, including the scaled covariance function $\xi_g(t, s)$, that are not invariant to time shifts.

The transformation of Eq. (1) exactly matches the target marginal distribution of $Z(t)$ since

$$\begin{aligned} P(Z(t) \le z) &= P(F_t^{-1} \cdot \Phi(Y(t)) \le z) \\ &= P(Y(t) \le \Phi^{-1} \cdot F(z, t)) = F(z, t). \end{aligned} \tag{2}$$

The finite dimensional distributions of $Z(t)$ are given, in terms of the d-dimensional multivariate Gaussian distribution $\Phi_d(\cdot)$, by

$$F_d(z_1, \ldots, z_d; t_1, \ldots, t_d) = \Phi_d(y_1, \ldots, y_d) \tag{3}$$

where $y_i = \Phi^{-1} \cdot F(z_i, t_i)$, $y_i = y(t_i)$ is the Gaussian image of $z(t_i)$. The finite dimensional joint probability density functions of $Z(t)$, which are obtained by direct differentiation of Eq. (3) are

$$\begin{aligned} f_d(z_1, \ldots, z_d; t_1, \ldots, t_d) &= \phi_d(y_1, \ldots, y_d) \prod_{r=1}^{d} \frac{f(z_r, t_r)}{\phi(y_r)} \\ &= \frac{1}{\sqrt{(2\pi)^d \det \xi_g}} \exp\left(-\frac{1}{2} \mathbf{y}^T \xi_g^{-1} \mathbf{y} \right) \prod_{r=1}^{d} \frac{f(z, t_r)}{\phi(y_r)} \end{aligned} \tag{4}$$

where $\mathbf{y} = [y_1, \ldots, y_d]^T$, $\phi(\cdot)$ is the univariate Gaussian density function and $\xi_{g,ij} = \xi_g(t_i, t_j)$ with $\xi_g(t, s)$ being the scaled covariance function of the underlying Gaussian random process $Y(t)$.

The second moment properties of $Z(t)$ are partially described by the scaled covariance function $\xi(t, s)$ which is related to the covariance function of the Gaussian process $Y(t)$ by

$$\begin{aligned} &\mu(t)\mu(s) + \sqrt{c(t, t)c(s, s)}\xi(t, s) \\ &= \int_{-\infty}^{\infty} \int_{-\infty}^{\infty} g(u, t) g(v, s) \phi(u, v; \xi_g(t, s)) \mathrm{d}u \, \mathrm{d}v \end{aligned} \tag{5}$$

in which $\phi(\cdot, \cdot, \xi)$ is the bivariate Gaussian density function with correlation coefficient ξ and $c(\cdot, \cdot)$ is the covariance function of $Z(t)$ so that $c(t, t) = \sigma(t)$ and $c(s, s) = \sigma(s)$, the standard deviations of $Z(t)$ and $Z(s)$. The scaled covariance of $Z(t)$ therefore depends upon the marginal distributions $F(z, t)$ and $F(z, s)$, as well as the correlation coefficient of the Gaussian random variables $Y(t)$ and $Y(s)$. Rearrangement of Eq. (5) leads to a definition of the correlation distortion function which is denoted here by $\xi(t, s) = h(\xi_g; t, s)$.

2.1. Properties of the correlation distortion function

The correlation distortion function is, for fixed t and s, a monotonically non-decreasing function of ξ_g. This is shown by use of Price's theorem [24] which states that

$$\begin{aligned} \frac{d}{\mathrm{d}\xi_g(t, s)} h(\xi_g; t, s) &= \frac{\partial \xi(t, s)}{\partial \xi_g(t, s)} \\ &= \frac{1}{\sqrt{c(t, t)c(s, s)}} E\left[\frac{d}{\mathrm{d}U} g(U, t) \frac{d}{\mathrm{d}U} g(U, s) \right]. \end{aligned} \tag{6}$$

The right hand side of Eq. (6) is non-negative, since $g(\cdot, t)$ is non-decreasing due the non-decreasing character of the inverse cdfs $F_t^{-1}(\cdot)$. Since the right hand side of Eq. (6) is non-negative, the correlation distortion function must be itself monotonically non-decreasing.

Since $h(\xi_g; t, s)$ is non-decreasing, and since $-1 \le \xi_g \le 1$, it must be bounded by

$$h(-1; t, s) \le h(\xi_g; t, s) \le h(1; t, s). \tag{7}$$

The scaled covariance of $Z(t)$, $\xi(t, s)$ is zero when $\xi_g(t, s)=0$. When $\xi_g(t, s)=0$, the Gaussian random variables $Y(t)$ and $Y(s)$ are independent so that the integral of Eq. (5) can be separated into

$$\xi(t,s) = \left[\int_{-\infty}^{\infty} g(u,t)\phi(u)\mathrm{d}u \int_{-\infty}^{\infty} g(u,s)\phi(u)\mathrm{d}u - \mu(t)\mu(s)\right] \times \frac{1}{\sqrt{c(t,t)c(s,s)}} = 0. \tag{8}$$

The upper and lower bounds on $\xi(t, s)$ can be calculated using Eq. (5). Evaluation of $h(-1; t, s)$, for which $\phi(u, v; -1)$ takes non-zero values only on the line $u=-v$, yields

$$\mu(t)\mu(s) + \sqrt{c(t,t)c(s,s)}\xi^{\min}(t,s) = \int_{-\infty}^{\infty} g(u,t)g(-u,s)\phi(u)\mathrm{d}u \tag{9}$$

or, written using the expectation operator,

$$\xi^{\min}(t,s) = \frac{E[g(U,t)g(-U,s)] - E[g(U,t)]E[g(U,s)]}{\sqrt{(E[g(U,t)^2] - E[g(U,t)]^2)(E[g(U,s)^2] - E[g(U,s)]^2)}} \tag{10}$$

The upper bound is obtained by an analogous calculation based on the fact that when $\xi_g=1$, the bivariate Gaussian density function takes non-zero values only for $u=v$. The upper bound is

$$\mu(t)\mu(s) + \sqrt{c(t,t)c(s,s)}\xi^{\max}(t,s) = \int_{-\infty}^{\infty} g(u,t)g(u,s)\phi(u)\mathrm{d}u \tag{11}$$

or, written using the expectation operator,

$$\xi^{\max}(t,s) = \frac{E[g(U,t)g(U,s)] - E[g(U,t)]E[g(U,s)]}{\sqrt{(E[g(U,t)^2] - E[g(U,t)])(E[g(U,s)^2] - E[g(U,s)])}}. \tag{12}$$

When at least one of the marginal cdfs $F(z, t)$ and $F(z, s)$ satisfy $F(-z,\cdot)=-F(z,\cdot)$, i.e. the function is odd, then

$$\xi(t,s)^{\min} = \frac{-E[g(U,t)g(U,s)]}{\sqrt{E[g(U,t)^2]E[g(U,s)^2]}} = -\xi(t,s)^{\max}. \tag{13}$$

This finding can be extended to the conclusion that if at least one of the marginal cdfs $F(z, t)$ and $F(z, s)$ is odd, then so is the correlation distortion function $h(\xi_g; t, s)$. Note that an equivalent statement of this condition can be done with g, since the standard Gaussian cdf $\Phi(\cdot)$ is an even function. The brief proof is given here assuming that $g(z, s)$ is odd, and, without loss of generality, that $Z(t)$ has mean zero and unit variance at all times. The steps to show this property are

$$\begin{aligned} h(-\xi_g; t, s) &= \int_{-\infty}^{\infty}\int_{-\infty}^{\infty} g(u,t)g(v,s)\phi(u,v;-\xi_g)\mathrm{d}u\,\mathrm{d}v \\ &= \int_{-\infty}^{\infty}\int_{-\infty}^{\infty} g(u,t)g(v,s)\phi(u,-v;\xi_g)\mathrm{d}u\,\mathrm{d}v \\ &= \int_{-\infty}^{\infty}\int_{-\infty}^{\infty} g(u,t)g(-v,s)\phi(u,v;\xi_g)\mathrm{d}u\,\mathrm{d}v \\ &= -\int_{-\infty}^{\infty}\int_{-\infty}^{\infty} g(u,t)g(v,s)\phi(u,v;\xi_g)\mathrm{d}u\,\mathrm{d}v \\ &= -h(\xi_g; t, s). \end{aligned} \tag{14}$$

For it to be possible to match a target scaled covariance function, the target function must satisfy two conditions. The first is that $\xi^{\min}(t, s)\le\xi(t, s)\le\xi^{\max}(t, s)$ for all pairs of time instants (t, s). The second is that the correlation function of the underlying Gaussian random process, defined in the inverse by $\xi(t, s)=h(\xi_g(t, s), t, s)$ must be non-negative definite. To be non-negative definite, the correlation function $\xi_g(t, s)$ must satisfy the condition that the matrix $\boldsymbol{\xi}_g(\mathbf{t})$, defined by $\xi_{g,ij}=\xi_g(t_i, t_j)$, be non-negative definite for all vectors $\mathbf{t}\in\mathbb{R}^n$ for any integer n. This condition is equivalent to the condition that $\mathbf{a}^T\boldsymbol{\xi}_g(\mathbf{t})\mathbf{a}\ge 0$, again, for all vectors $\mathbf{t}\in\mathbb{R}^n$ for any integer n. An alternative condition is that $\lambda_1(\boldsymbol{\xi}_g(\mathbf{t}))\ge 0$, where λ_1 is the smallest eigenvalue of $\boldsymbol{\xi}_g(\mathbf{t})$. The condition of non-negative definiteness is practically difficult to check using these conditions because of the requirement that the conditions hold for all $\mathbf{t}\in\mathbb{R}^n$ for any integer n.

An alternative method for checking non-negative definiteness of the Gaussian correlation function relies on the spectral density function defined for a mean zero unit variance process by

$$S(\omega_1,\omega_2) = \int_{-\infty}^{\infty}\int_{-\infty}^{\infty} \xi(t,s)\mathrm{e}^{\mathrm{i}2\pi(\omega_1 t-\omega_2 s)}\mathrm{d}t\,\mathrm{d}s. \tag{15}$$

If the correlation function $\xi_g(t, s)$ is non-negative definite then the spectral density function satisfies $S(\omega_1, \omega_2)\ge 0$ $\forall(\omega_1, \omega_2)\in\mathbb{R}^2$. Finally, the requirement of a non-negative definite covariance function implies that there may be a significant restriction on the range of possible correlation functions that can be achieved by translation. Some discussion of this issue is provided in [17]. In the following sections, the feasibility of the theoretical extension into non-stationary translation will be shown through practical examples.

2.2. Parametrization of marginal cdfs

In the above description of the properties of non-stationary processes, the correlation distortion function depends on the correlation value ξ_g of the underlying Gaussian random process $Y(t)$ and two time arguments t and s. For generation of long samples, such a definition requires

extensive computation, in that Eq. (5) must be solved inversely, usually by numerical approximation, for the range of values $\xi_g \in [-1, 1]$ and $t, s \in [0, t_f]$ if the process starts at $t=0$ and ends at $t=t_f$. If the marginal cdfs of $Z(t)$ depend upon a finite set of parameters, which themselves are defined over a finite range, the calibration of the correlation function can be simplified significantly. Let $F(z, t) = F(z, \boldsymbol{\lambda}(t))$, where $\boldsymbol{\lambda}(t)$ is an n-dimensional vector containing the parameters of the distribution. An example would be the upper and lower bounds of a uniform distribution. If the marginal cdfs can be so parametrized, then the correlation distortion function can be written as

$$h(\xi_g; t, s) = h(\xi_g; \boldsymbol{\lambda}(t), \boldsymbol{\lambda}(s)). \tag{16}$$

The correlation distortion function can thus be defined on the $2n+1$ dimensional space in which the coordinate axes are the scaled covariance $\xi_g(t, s)$, and the components of $\boldsymbol{\lambda}(t)$ and $\boldsymbol{\lambda}(s)$. If this space is finite, then a finite number of nodal points can be defined at which Eq. (5) is evaluated. Provided a fine enough discretization, the correlation distortion function can be approximated by interpolation of these nodal values. Since the correlation distortion function is in general quite smooth, a fairly coarse discretization of the $(\xi_g, \boldsymbol{\lambda}(t), \boldsymbol{\lambda}(s))$ space will often provide satisfactory results. Calibration of the correlation function $\xi_g(t, s)$ of $Y(t)$ can then be carried out as follows:

1. Discretize the (t, s) space on which $\xi_g(t, s)$ is defined with a set of nodal points;
2. For each nodal point (t_i, s_j), find $\boldsymbol{\lambda}(t_i)$ and $\boldsymbol{\lambda}(s_j)$;
3. Given the known target value of ξ, perform a multi-dimensional table lookup and interpolation to find the correct value of ξ_g.

3. Monte Carlo simulation

If $F(z, t)$, and $\xi(t, s)$ are the marginal distribution and scaled covariance function of the process $Z(t)$ that is to be modeled by a non-stationary translation process, the definitions above provide a straightforward method for generating realizations of $Z(t)$ on the interval $[0, t_f]$.

The first step is to determine the underlying Gaussian correlation function $\xi_g(t, s)$. In rare cases, it may be possible to solve Eq. (5), an inverse equation, analytically. In most cases, however, $\xi_g(t, s)$ must be determined numerically. One possible procedure is to define an $n \times m$ grid of points $\{t_i, s_j\}$, $i=1,\ldots,n$, $j=1,\ldots,m$ in the space $[0, t_f]^2$, and a set of correlation values $\{\rho_k\}$, $k=1,\ldots,l$ in the range $[-1, 1]$ and evaluate all $\xi_{kij} = \xi(\rho_k, t_i, s_j) = h(\rho_k, t_i, s_j)$. An approximate, discretized version of $\xi_g(t, s)$ can be obtained by interpolating the values ξ_{kij}. This interpolation can be accomplished rapidly using, for example, the built-in `MATLAB` function `interp2`.

Once the correlation function of the underlying Gaussian process is determined generation of samples of $Z(t)$ requires only the generation of samples of $Y(t)$, the underlying Gaussian process. These samples can be generated in a variety of ways ([2–5] and [6]). Two alternative methods rely on the definition of a set of nodes t_i $i=1,\ldots,n$, $t_i \in [0, t_f]$ that are ordered so that $t_i < t_{i+1}$. The process $Y(t)$ is approximated by its nodal values $Y_i = Y(t_i)$.

If the sample to be generated is not very long, and can be represented with sufficient accuracy by a few thousand nodal points, then the nodal values $\{Y_i\}$ can be arranged into a vector $\mathbf{Y}$ whose components are the nodal values of the process. This mean zero, unit variance, Gaussian random vector, has correlation matrix $\boldsymbol{\xi}_g$ whose components are defined by $\xi_{g,ij} = \xi_g(t_i, t_j)$. Samples of this Gaussian vector can be generated efficiently using the Cholesky decomposition $\boldsymbol{\beta}(\boldsymbol{\xi}_g)$ by the matrix operation $\mathbf{Y} = \boldsymbol{\beta}\mathbf{Z}$, where $\mathbf{Z}$ is a mean zero, unit variance, Gaussian random vector with uncorrelated components [24]. Alternatively, the Modal decomposition $\boldsymbol{\Psi}(\boldsymbol{\xi}_g)$ by the matrix operation $\mathbf{Y} = \boldsymbol{\Psi}\mathbf{Z}$, where $\boldsymbol{\Psi}$ contains the eigenvectors of $\boldsymbol{\xi}_g$, can also be used [25]. Either approach can be implemented as long as the number of nodal points is not too large. On a typical desktop computer, vectors of several thousand components can be efficiently simulated using this method.

At some number of nodal points the calculation of the matrix $\boldsymbol{\beta}$ (or $\boldsymbol{\Psi}$) becomes overly time consuming. If the desired sample length is too long, or requires too many nodal points to allow for simulation by the above method, a simulation method based on conditional random vectors can be used. The nodal value Z_i is treated as the conditional random variable $Z_i | Z_{i-m} = z_{i-m}, \ldots, Z_{i-1} = z_{i-1}$ where m is the window size and should satisfy $m\Delta t \geq l_c$ where $\Delta t = |t_i - t_{i-1}|$ is the nodal spacing and l_c is the correlation length of the $Z(t)$. Generation of this conditional Gaussian variable can be accomplished by using directly the properties of Gaussian random vectors [26]. In all examples shown in this paper, sample generation is accomplished using the Cholesky or Modal decomposition method described above.

4. Example

In order to demonstrate the technique described in the previous section, three non-stationary examples will be provided here: a uniformly distributed process, a lognormally distributed process and a binary process. In all cases, the non-stationarity is manifested by the time dependence of the marginal pdf $f(z, t)$ that can be parametrized.

4.1. Non-stationary uniformly distributed process

Let $Z(t)$ be a non-stationary uniformly distributed process. The parameters of the distribution $F(z, \boldsymbol{\lambda}(t))$, contained in $\boldsymbol{\lambda}(t)$, are the upper and lower range values $b(t)$ and $a(t)$ of $Z(t)$.

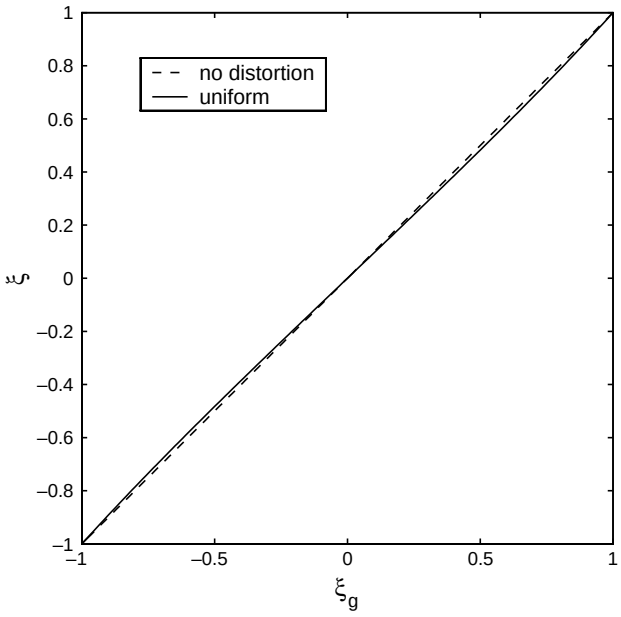

Fig. 2. Correlation distortion function for a translation process with uniformly distributed CDF, calculated numerically from Eq. (18).

The translation process of Eq. (1) is then written as:

$$Z(t) = g(Y(t), t) = a(t) + (b(t) - a(t))\Phi(Y(t)) \tag{17}$$

The correlation distortion function described in Eq. (5) can therefore be simplified to:

$$\xi = h(\xi_g, t, s)$$

$$= 12 \int_{-\infty}^{\infty} \int_{-\infty}^{\infty} \Phi(u)\Phi(v)\phi(u, v; \xi_g(t, s))\mathrm{d}u\ \mathrm{d}v - 3 \tag{18}$$

For which a closed form solution has been derived by [27], and used in [28] for rank-based simulation:

$$\xi = h(\xi_g, t, s) = \frac{6}{\pi} \arcsin\left(\frac{\xi_g(t, s)}{2}\right) \tag{19}$$

Note that, for this particular non-stationary translation, $h(\cdot, t, s)$ is independent of the parameters $\boldsymbol{\lambda}(t)$ and $\boldsymbol{\lambda}(s)$. Also, it can be easily shown that the upper and lower bounds of Eqs. (9) and (11) correspond to $\xi^{\min}(t, s) = -1$ and $\xi^{\max}(t, s) = 1$ for all points t, s, indicating that all values of ξ within the range $[-1, 1]$ match one-to-one ξ_g values. Both properties are connected to the fact that the uniform pdf belongs to the group of distributions that can be reduced to a standard form (where $a = 0$, $b = 1$)through a linear transformation [29]. Another significant feature of Eq. (18) is the considerably small correlation distortion observed along the range $-1 < \xi(\xi_g) < 1$, as shown in Fig. 2. For simulation purposes, this low distortion also provides a quick and efficient way to generate a vector with any mean and standard deviation as input information.

As an example, assume the process $Z(t)$ discretized to three points Z_1, Z_2, Z_3 with the means and standard deviations μ_1, $\sigma_1 = (0.5, 1.5)$, μ_2, $\sigma_2 = (2, 0.5)$ and μ_3, $\sigma_3 = (4, 1)$, and with the target correlation coefficients of $\xi_{12}^T = 0.2$, $\xi_{13}^T = -0.4$ and $\xi_{23}^T = 0.5$. Following the above discussion, all values of correlation between the range $-1 \leq \xi_{kl}^T \leq 1$ for k, $l = 1$–3 and $k \neq l$, can be achieved through $Z_i = F_i^{-1}(\Phi(Y_i))$, where F_i corresponds to the marginal uniform cdf of Z of component i. Therefore, the components of Z will be perfectly correlated when the underlying Gaussian components are perfectly correlated.

Since the correlation distortion function in Eq. (18) depends only on ξ_g, it is straightforward to interpolate the non-Gaussian target correlation values ξ_{kl}^T to calculate their Gaussian equivalents $\xi_{g,kl}^T$, which are obtained as $\xi_{g,12}^T = 0.209$, Journal of the Physiological Society of Japan and $\xi_{g,23}^T = 0.518$. These are the target correlation values required for the underlying Gaussian vector in order to obtain the target non-Gaussian correlations defined above. The distortion is very small in this case, but this interpolation procedure will also be used in subsequent examples, where distortion can be significantly higher.

Although not shown, there is very close agreement between the target marginal pdfs and the histograms of 10, 000 samples of Z_1, Z_2 and Z_3. For comparison, both Gaussian and non-Gaussian correlation values of the simulated samples is compared versus their target values in Table 1. While the difference between target and simulated values is almost negligible for practical purposes, interpolation through $\xi_{g,kl} = h^{-1}(\xi_{kl}^T)$ provides consistently lower absolute errors ($\simeq 0.3\%$) when compared to samples generated where distortion is not considered (i.e. $\xi_{g,kl} = \xi_{kl}^T$) where the error obtained is around 3.0%.

This example demonstrates the application of sets of random variables to non-stationary, non-Gaussian translation processes. In this case, the degree of correlation distortion found after using the translation in Eq. (17) is small, as is the number of random variables. The extension of the technique to non-stationary processes with significant correlation distortion and larger numbers of sampling points is straightforward and will be shown in the next two examples.

Table 1
Target and ensemble correlation values for a uniformly distributed translation process

k, l	Target (ξ_{kl}^T)	Gaussian ($\xi_{g,kl} = h^{-1}(\xi_{kl}^T)$)	Ensemble (ξ_{kl})	Gaussian ($\xi_{g,kl} = \xi_{kl}^T$)	Ensemble (ξ_{kl})
1, 2	0.200	0.209	0.200	0.200	0.210
1, 3	−0.400	−0.416	−0.403	−0.400	−0.421
2, 3	0.500	0.518	0.497	0.500	0.511

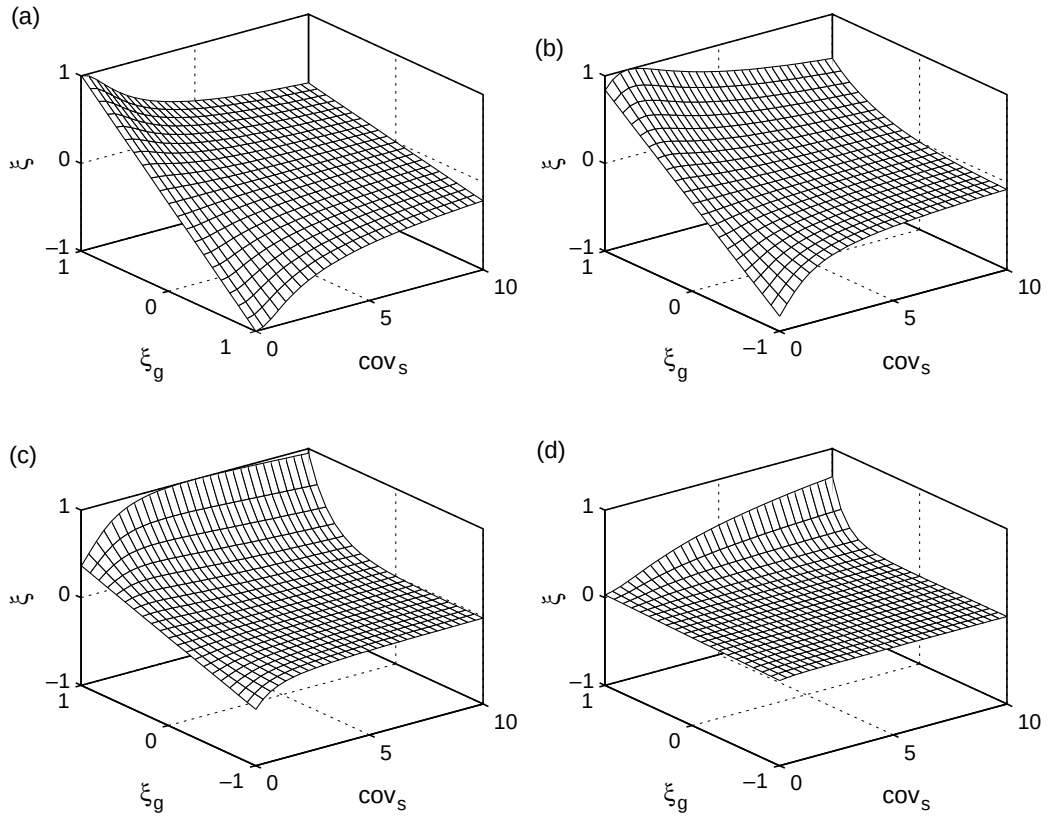

Fig. 3. Distortion correlation plots in the domain as a function of underlying Gaussian correlation ξ_g and coefficient of variation at point s, cov_s for (a) $\mathrm{cov}_t = 0.01$, (b) $\mathrm{cov}_t = 1$, (c) $\mathrm{cov}_t = 5$ and (d) $\mathrm{cov}_t = 100$ of a non-stationary lognormally distributed translation process.

4.2. Non-stationary lognormal distributed process

This example highlights the application of non-stationary translation processes to simulation of random processes with a higher level of correlation distortion. Assume the following form of the translation for Eq. (1):

$$Z(t) = g(Y(t), t) = \exp(\mu(t) + \sigma(t)Y(t)) \tag{20}$$

In this case, $\mu(t)$ and $\sigma(t)$ are the time-varying mean and standard deviation of $\log(z)$. For such a translation, the marginal cdf at each step t corresponds to a lognormal cdf:

$$F_t(t) = F(z, t) = \Phi\left(\frac{\log(z) - \mu(t)}{\sigma(t)}\right) \tag{21}$$

where $\log(\cdot)$ is the natural logarithmic function. Furthermore, it is important to note that $\mu(t)$ and $\sigma(t)$ are not the mean and standard deviation of $Z(t)$ but rather the log $(Z(t))$. Hence, in order to prescribe target values with respect to t in the non-Gaussian domain, it is necessary to define the relationship $(\mu_z(t), \sigma_z(t)) = f(\mu(t), \sigma(t))$ that maps the transformation between both parameters. For lognormal random variables, this relationship is readily available and can be used in conjunction with the definition of $g(Y(t), t)$ to find the correlation distortion. Performing this substitution, it can be shown that the correlation distortion function is only dependent on the coefficient of variation $\mathrm{cov}(t)$, where $\mathrm{cov}(t) = \mathrm{cov}_t = \sigma_z(t)/\mu_z(t)$ represents the lognormal coefficient of variation at time instant t. Hence, Eq. (5) can then be derived in the parametric

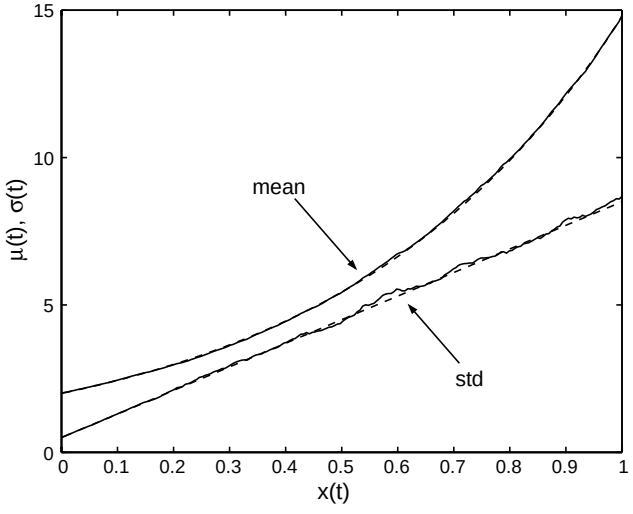

Fig. 4. Target (dashed) and ensemble (solid) mean and standard deviation for 10,000 samples of a non-stationary lognormal translation process with exponentially correlated components.

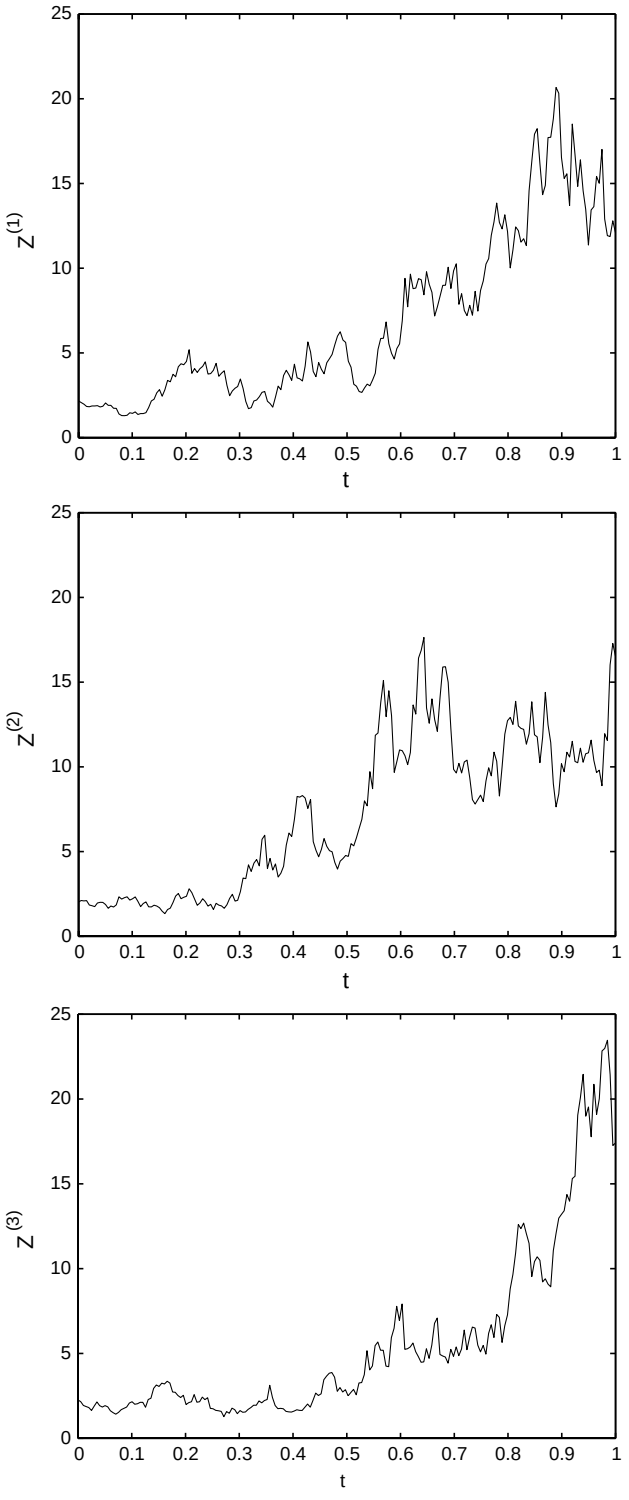

Fig. 5. Three samples of a non-stationary lognormal translation process with first order properties defined in Eq. (23) and exponentially correlated components.

form $h(\xi_g;\ \boldsymbol{\lambda}(t),\ \boldsymbol{\lambda}(s)) = h(\xi_g;\ \mathrm{cov}(t),\ \mathrm{cov}(s))$:

$$\xi(t,s) = \frac{\exp(\xi_g\sqrt{\log(\mathrm{cov}(t)^2+1)\log(\mathrm{cov}(s)^2+1)}) - 1}{\mathrm{cov}(t)\mathrm{cov}(s)} \tag{22}$$

In order to visualize the correlation distortion function, ξ is plotted against ξ_g for a series of fixed values of cov_t and a range of cov_s, as shown in Fig. 3. As $\mathrm{cov}_t \to 0$ and $\mathrm{cov}_s \to 0$ (i.e. deterministic case), no distortion is observed for the range $\xi_g = [-1,1]$ since $\xi = \xi_g$. Furthermore, perfect correlation is always achieved at $h(\xi_g = 1;\ t,\ s) = 1$ when $\mathrm{cov}_t = \mathrm{cov}_s$, i.e. when stationary. However, unlike the previous example, the simulated non-Gaussian non-stationary process $\mathbf{Z}$ will not always match perfect correlation ($\xi \neq 1$) for $\xi_g = 1$, nor will it always match perfectly negative correlation ($\xi \neq -1$) for $\xi_g = -1$. This inability to match perfectly negative correlation is also observed in the stationary case when $\mathbf{Z} = \exp(\mathbf{Y})$ [10]. Therefore, the process can only be simulated if the target values of ξ are defined within the limits $\xi^{\max}(t,\ s)$ and $\xi^{\min}(t,\ s)$ for the domain $[\mathrm{cov}_t,\ \mathrm{cov}_s] \times [\mathrm{cov}_t,\ \mathrm{cov}_s]$.

As an example, let $\mathbf{Z}$ be a discretized non-stationary random vector with components Z_i, $i = 1,\ldots,200$ obtained with an exponential translation where the mean and standard deviation are chosen to vary according to the following

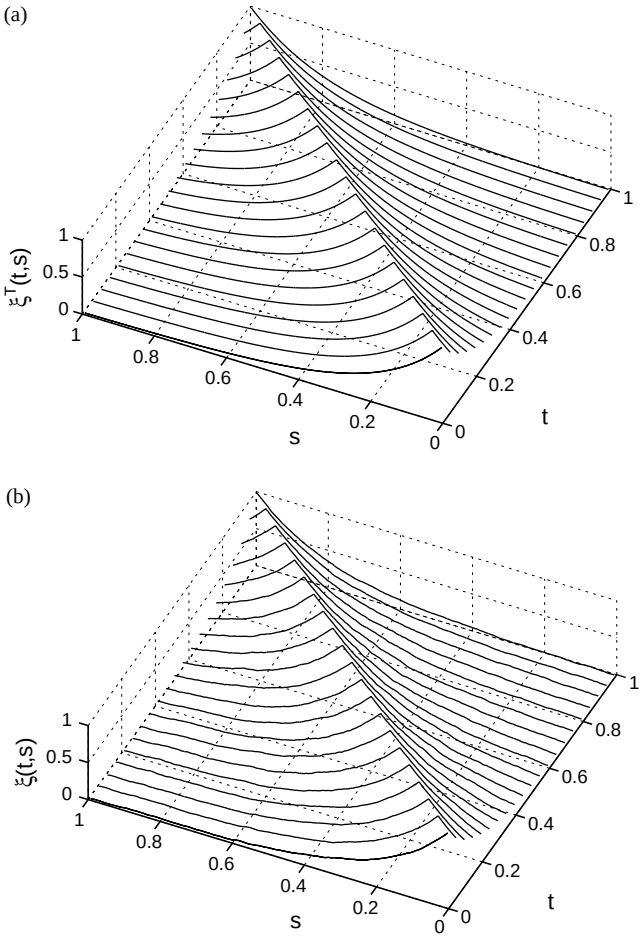

Fig. 6. Comparison between (a) target exponentially decaying correlation $\xi^T(t,\ s)$ with $\tau_0 = 0.4$ and (b) ensemble correlation $\xi(t,\ s)$ of 10,000 samples of a lognormal translation process.

equations:

$$\mu(t) = 2(e^t)^2, \quad \sigma(t) = 8t + \frac{1}{2} \tag{23}$$

where the coordinate t is discretized between 0 and 1. This will result in a process whose mean increases according to Eq. (23) from 2 to 14.78, with a linearly varying standard deviation between 0.5 and 8.5. The correlation between each component of $\mathbf{Z}$ is chosen to vary according to an exponentially decaying function:

$$\xi^T(t,s) = \left[\exp\left(\frac{|z(t) - z(s)|}{\tau_0}\right)\right]^2 \tag{24}$$

where τ_0 is the correlation distance of the process, chosen in this case to be $\tau_0 = 0.4$. From the target correlation defined by Eq. (24), interpolation is carried out using a finite set of numerically computed nodal points $h(n_{ijk})$ for a range $[0,1]\times[\mathrm{cov}_t, \mathrm{cov}_s]\times[\mathrm{cov}_t, \mathrm{cov}_s]$ that includes the correlation space of $\mathbf{Z}$, in order to find the Gaussian correlation function $\xi_{g,ij}$. Then, 10,000 samples of the Gaussian vector Y_i, $i = 1,\ldots,200$ are obtained using modal decomposition. Each vector Y_i is then converted to Z_i using the expression in Eq. (20), leading to 10,000 samples of $\mathbf{Z}$. The ensemble mean and ensemble standard deviation for these samples is shown to match the target values very closely in Fig. 4. Three samples from these ensemble are shown in Fig. 5. Also, both target ξ^T and simulated ξ correlation functions are compared in Fig. 6, again with very good agreement. The maximum absolute difference for the whole domain is around 3.5%. Although not shown, marginal pdfs for each component of $\mathbf{Z}$ show almost exact agreement with the target lognormal distributions with mean and standard deviations corresponding to Eq. (23).

4.3. Simulation of statistically inhomogeneous random media

Many engineering applications require a combination of material properties that may not be feasible in typical one-phase materials. In some cases, this combination will

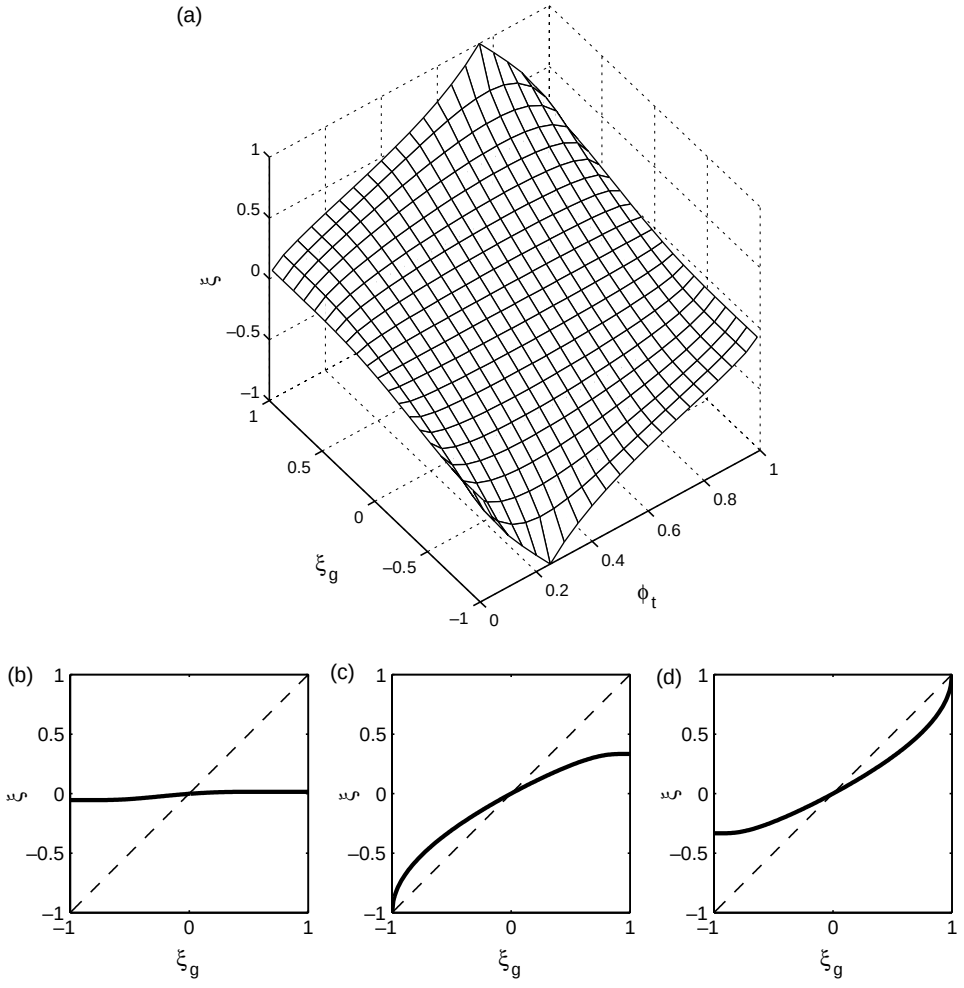

Fig. 7. Distortion correlation plot for $\phi_s = 0.75$ in (a) the domain $[-1,1]\times[\xi_l^{\min}, \xi_l^{\max}]\times[\phi_l, \phi_u]$, (b) $\phi_t = 0.01$, (c) $\phi_t = 1 - \phi_s$ and (d) $\phi_t = \phi_s$ for a non-stationary binary process.

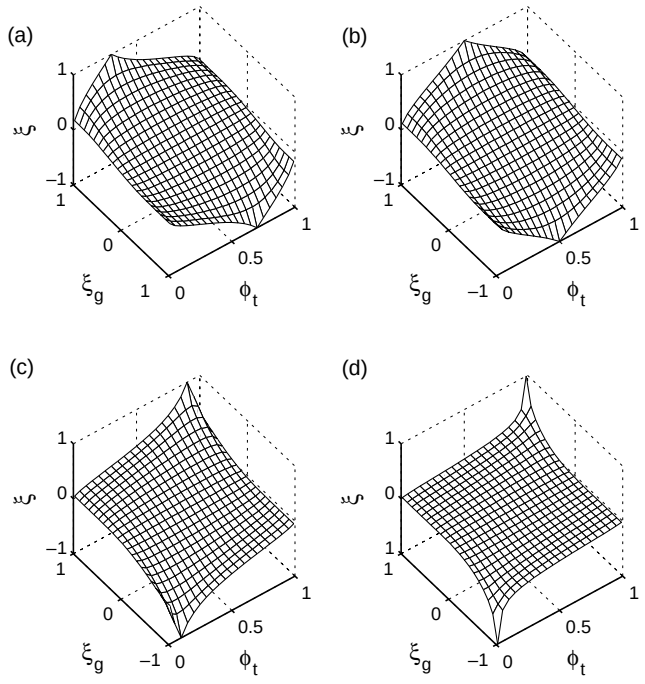

Fig. 8. Distortion correlation plots in the domain $[-1,1]\times[\xi_l^{\min},\xi_l^{\max}]\times[\phi_l,\phi_u]$ for (a) $\phi_s=0.3$, (b) 0.5, (c) 0.9 and (d) 0.99 for a non-stationary binary process.

also depend on the location of a particular component. For example, the exterior of a turbine blade or engine that is exposed to high temperatures must be able to shield its components from the extreme environment, while the interior must provide sufficient structural strength. Composites with a graded profile in microstructure and/or composition, titled functionally graded materials (FGMs), have been studied and developed as possible solutions for such cases in recent years ([30–33] to name a few).

Unlike traditional composites, these heterogeneous materials exhibit a gradual transition between two or more phases, producing a continuous variation in the physical characteristics of the composite at the macroscopic or continuum level. Such gradation can also be observed in some biological materials, such as bamboo and bone. An illustration of a two-phase material with locally varying composition is shown in Fig. 1.

Such a composite can exhibit considerable variation in material properties due to manufacturing complexity and statistical inhomogeneity. Therefore, characterization of the local volume fraction or material properties can be a particularly attractive application of non-Gaussian, non-stationary translation processes.

4.3.1. Non-stationary binary distributed process

In order to simulate statistically inhomogeneous two-phase random media, a non-stationary binary translation is developed. If the two phases occupy disjoint subdomains $V^{(1)}(\mathbf{t})$ and $V^{(2)}(\mathbf{t})$ (with $V^{(1)}(\mathbf{t})\cup V^{(2)}(\mathbf{t})=V$ and $V^{(1)}(\mathbf{t})\cap V^{(2)}(\mathbf{t})=\varnothing$) in $V\in\mathbb{R}^n$, the material can be represented by a characteristic function

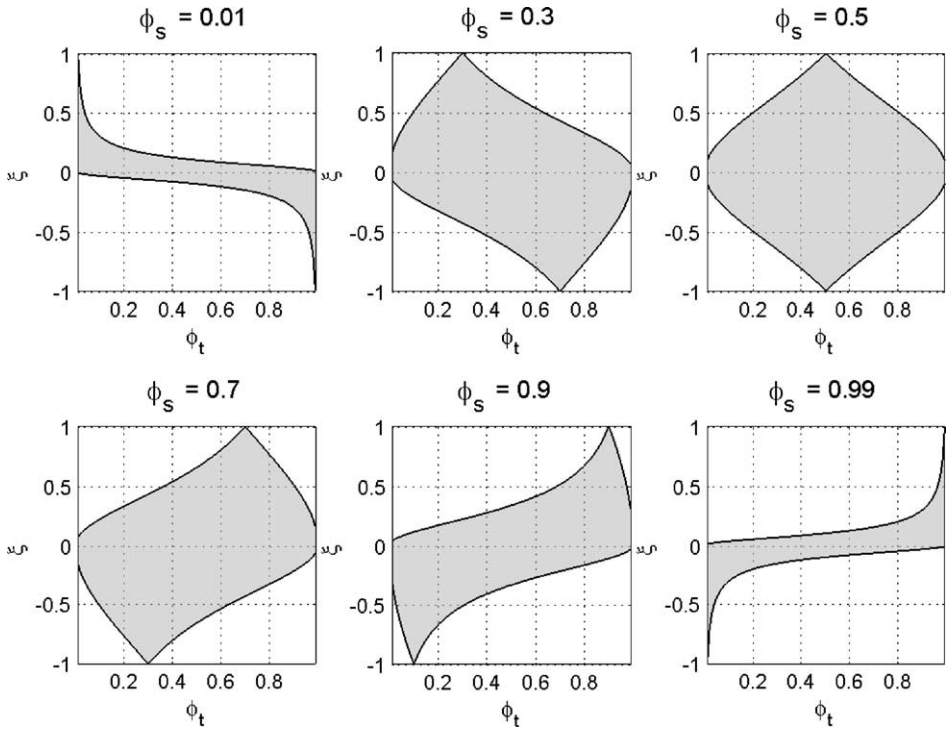

Fig. 9. Region of achievable non-Gaussian correlation values ξ for a non-stationary binary process for different fixed values of ϕ_s and a range of ϕ_t. Upper and lower bounds are defined by $\xi^{\max}(t,s)$ and $\xi^{\min}(t,s)$.

$$I(\mathbf{t}) = \begin{cases} 1, & \mathbf{t} \in V^{(1)}(\mathbf{t}) \\ 0, & \mathbf{t} \notin V^{(1)}(\mathbf{t}) \end{cases} \tag{25}$$

that is related to the phase volume fraction through the expectancy of the characteristic function, $\phi(\mathbf{t}) = E[I(\mathbf{t})]$. A memoryless translation is developed with the objective of matching both marginal probability density function and second order moment properties for a statistically inhomogeneous binary process. This is essentially done through non-stationary level cuts of Gaussian processes (or fields) as defined by:

$$Z_i(\mathbf{t}) = F_i^{-1} \circ \Phi(Y(\mathbf{t})) = \begin{cases} 1, & \text{if} \quad Y_i(\mathbf{t}) > c_i(\mathbf{t}) \\ 0, & \text{if} \quad Y_i(\mathbf{t}) \leq c_i(\mathbf{t}) \end{cases} \tag{26}$$

where $\mathbf{Y}$ is an underlying Gaussian process with mean zero and standard deviation equal to one. The limit $c(\mathbf{t})$ is related to the volume fraction by $\phi(\mathbf{t}) = P[Y(\mathbf{t}) > c(\mathbf{t})]$, where $\phi^1(\mathbf{t}) = V^{(1)}(\mathbf{t})/V$ and $\phi^{(2)}(\mathbf{t}) = 1\text{-}\phi^{(1)}(\mathbf{t})$. In order to match the target autocorrelation $\xi^T(t, s)$, Eqs. (5) and (26) are used to derive the correlation distortion function $h(\xi_g, \phi(t), \phi(s))$ numerically from:

$$\xi_{ij} = \frac{\int_{c_i}^{\infty} \int_{c_j}^{\infty} \phi(u, v; \xi_{g,ij}) \mathrm{d}u \, \mathrm{d}v - \phi_i \phi_j}{\sqrt{\phi_i(1-\phi_i)}\sqrt{\phi_j(1-\phi_j)}} \tag{27}$$

where $\phi(u, v, \xi_{g,ij})$ is the second order joint Gaussian probability density function. Plots of correlation distortion for the above equation are shown in Fig. 7, for a fixed value of $\phi_s = 0.75$. In the extreme cases when $\phi_t \to 0$ and $\phi_s \to 0$, results indicate that a very limited range of correlations can be obtained for the range $[-1,1]$ of ξ_g. This makes physical sense in that if a point on the sample has either a value of 0 or 1 with 100% probability, then it has no impact on (or correlation to) any other value in the microstructure. Furthermore, note in Fig. 7 that $\xi^{\max} = 1$ at $h(1, \phi_s, \phi_s)$ and $\xi^{\min} = -1$ at $h(-1, \phi_s, 1-\phi_s)$. These observations are directly reflected by the possible range of correlation values $[\xi^{\min}, \xi^{\max}]$ at each location t, s as shown in Fig. 8, for other fixed values of ϕ_s.

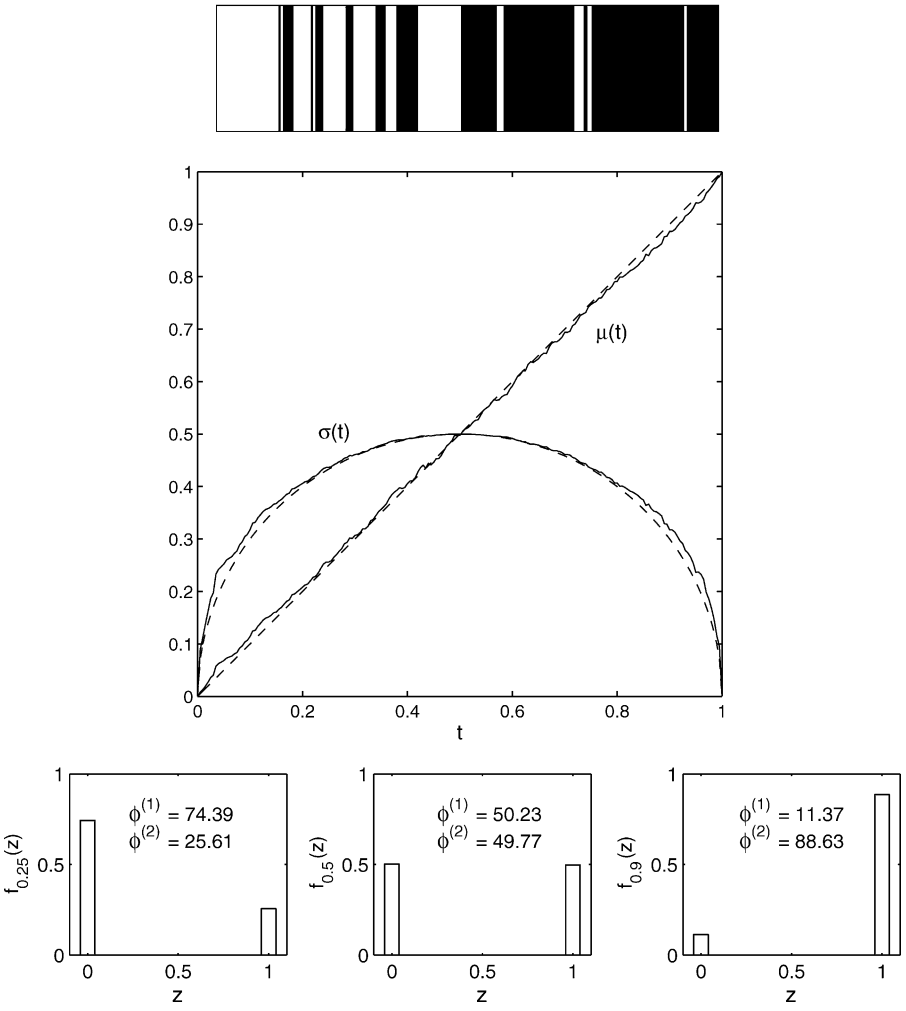

Fig. 10. Binary sample for case *A*, along with corresponding ensemble mean and standard deviation plotted against target values (dashed line) and marginal density functions at $t = 0.25$, 0.50 and 0.90 with ξ_A, where $\tau_0 = 0.03$.

As in the previous translation examples, simulation of a non-stationary binary process is still achievable through translation within the limiting $\xi^{\min}(t, s)$ and $\xi^{\max}(t, s)$ values. Due to the fact that this limitation is directly connected to the non-stationarity of the volume fraction, translation seems particularly suitable for this type of simulation. Using Eqs. (9) and (11), the lower and upper bounds can be obtained numerically as shown in Fig. 9.

4.3.2. Simulation of a 1D binary translation process

Let **Z** be a discretized non-stationary binary process with components Z_i varying along a normalized position $t \in [0,1]$ along the gradation coordinate $i = 1,\ldots,200$; representing a two-phase random media graded composite. Using the model described in the previous section, the mean and standard deviation depend on the prescribed variation of the volume fraction, according to:

$$\mu(t) = \phi(t), \quad \sigma(t) = \sqrt{\phi(t)(1-\phi(t))} \tag{28}$$

For this particular example $\phi(t)$ is chosen to vary from 0 to 1, similar to the pattern shown in Fig. 1, according to the following functional form

$$\phi(t) = \begin{cases} (1-t)^{1/m}, & \text{if } m < 1 \\ 1 - t^m, & \text{if } m \geq 1 \end{cases} \tag{29}$$

where m is a constant that controls the volume fraction variation. Two different types of autocorrelation functions will be prescribed for **Z**:

$$\text{Case } A : \xi_A(t,s) = \begin{cases} 1 - \dfrac{|t-s|}{\tau_0}, & |\tau| < \tau_0 \\ 0, & \text{elsewhere} \end{cases} \tag{30}$$

$$\text{Case } B : \xi_B(t,s) = \exp\left(-\frac{|t-s|}{\tau_0}\right) \tag{31}$$

where τ_0 is the correlation distance of the stochastic process **Z** for the correlation functions ξ_A (linear) and ξ_B (exponential). In this case, the first step for simulation is to map the $\xi^T(t, s)$ into $\xi_g^T(t,s)$ through the interpolating technique described previously. An underlying Gaussian process **Y** can then be simulated through a variety of techniques, to be translated into the non-stationary, binary process **Z** using Eq. (26).

The main limitation of this approach is that the upper and lower bounds discussed in the previous section must be observed by the choice of $\xi^T(t, s)$. This implies that τ_0 must be low in order to enforce this condition. From the physical constraints of the material, very high correlation lengths along t would also be unrealistic, since this can contradict the volume fraction variation described by Eq. (28). In other words, the length scale of the local volume fraction grading should be at least smaller than the length scale of the entire system to be physically reasonable. Hence, with these two conditions in mind, values of τ_0 are chosen accordingly, in order to reflect the length scale of the gradation and to define $\xi^T(t, s)$ within the bounds $\xi^{\min}(t, s)$ and $\xi^{\max}(t, s)$ for each correlation.

Samples and comparison with target values for the correlation function, marginal probability distributions, mean and standard deviation are shown in Figs. 10–13 for correlation functions ξ_A and ξ_B. The target inputs are matched very closely with the samples exhibiting gradation along t. The only case that shows slight discrepancies in the mean and standard deviation is the one corresponding to the linear correlation (case A). This is due to the fact that when $\xi_A(t, s)$ is mapped into $\xi_{g,A}(t, s)$, its Gaussian counterpart will have a spectral density function with negative values, as shown in Fig. 14. Therefore, it must be truncated for effective use in simulation, which, in turn, causes some small inaccuracies in the ensemble values.

The form of $\xi^{\min}(t, s)$ and $\xi^{\max}(t, s)$ discussed in the previous section (see Fig. 9) suggests that assuming a non-stationary target correlation might be more compatible with the probabilistic information of the stochastic process **Z**. To illustrate this approach, assume ξ^T corresponds to the

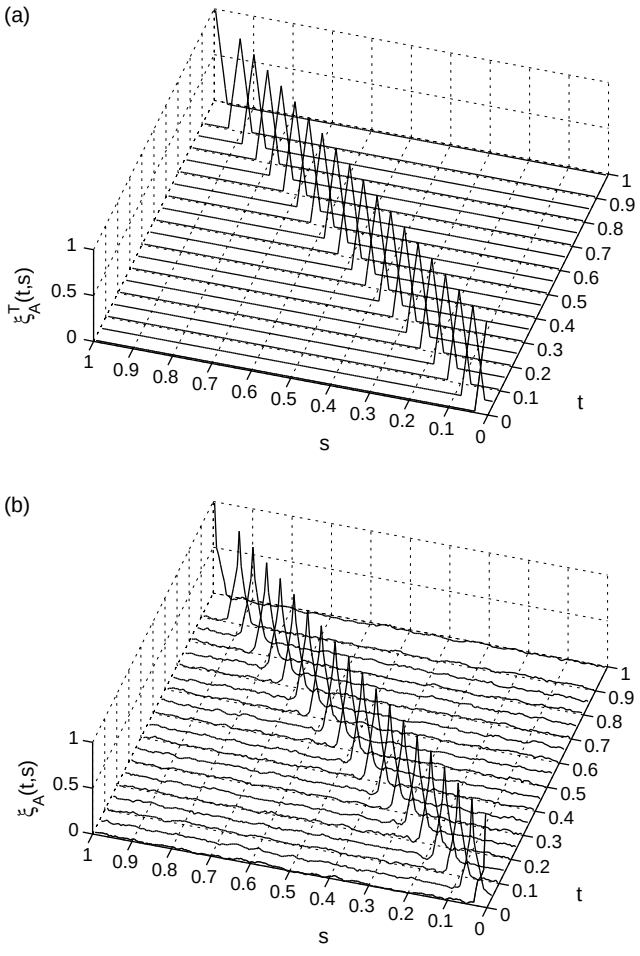

Fig. 11. Correlation function comparison for case A between (a) target and (b) ensemble of 10,000 samples of **Z** for ξ_A, where $\tau_0 = 0.03$.

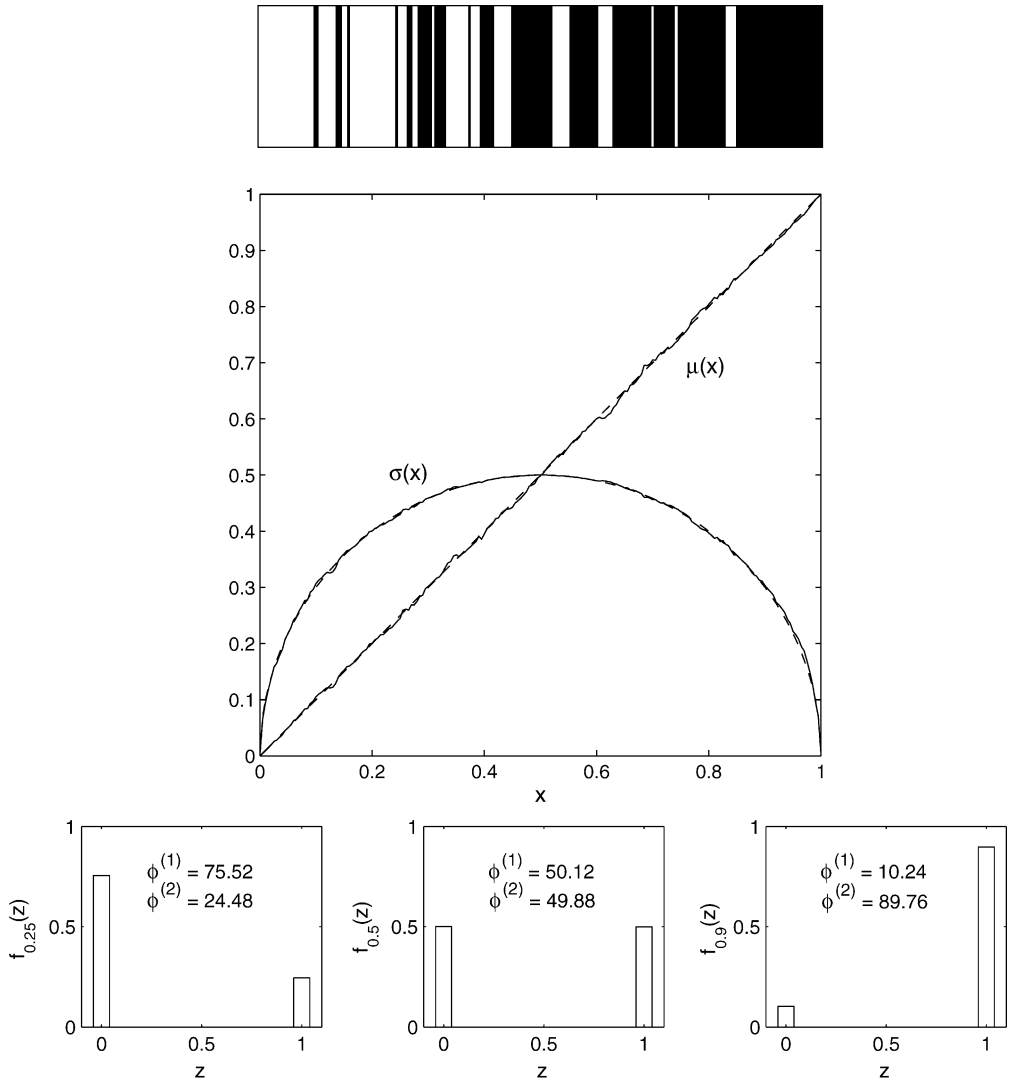

Fig. 12. Binary sample for case *B*, along with corresponding ensemble mean and standard deviation plotted against target values (dashed line) and marginal density functions at $t=0.25$, 0.50 and 0.90 with ξ_B, where $\tau_0=0.03$.

translation of a Gaussian exponential correlation ξ_g^T (see Eq. (31) with $\tau_0=0.4$). The contour plots of $\xi_{g,A}^T$ and ξ_A^T in Fig. 15 indicate that ξ^T exhibits a considerable non-stationary pattern when mapped through $h(\xi_g^T, s, t)$. Note that smaller values of τ_0 produce less non-stationarity, which could then be approximated as stationary if the resulting discrepancies are within reasonable tolerance.

Sample binary processes with this correlation function are given in Fig. 16, with 2000 points per sample and based on $\tau_0=0.05$. Three different values of m in Eq. (29) are used to show the effects of the volume fraction variation pattern. All three samples in 16 are developed from the underlying Gaussian process $\mathbf{Y}$.

5. Conclusion

Simulation of non-stationary, non-Gaussian stochastic vectors is achieved via translation mapping. The non-stationarity is directly connected to temporally or spatially varying marginal pdfs that represent a generalization of the stationary non-linear mapping of underlying Gaussian processes. The properties for this translation method indicate that upper and lower bounds limit the achievable target correlation values. However, application examples with different types of correlation functions and marginal pdfs show that exactly matching prescribed probabilistic information can be achieved.

An approach to Monte Carlo simulation using an interpolating technique in order to account for correlation distortion is discussed. This distortion arises from the non-linear nature of the transformation and its presented in a context that takes the temporal dependence into account. Furthermore, a parametrization of the cdf that improves the computational efficiency of the discretization required for the interpolating algorithm is introduced. The method can be easily implemented with any

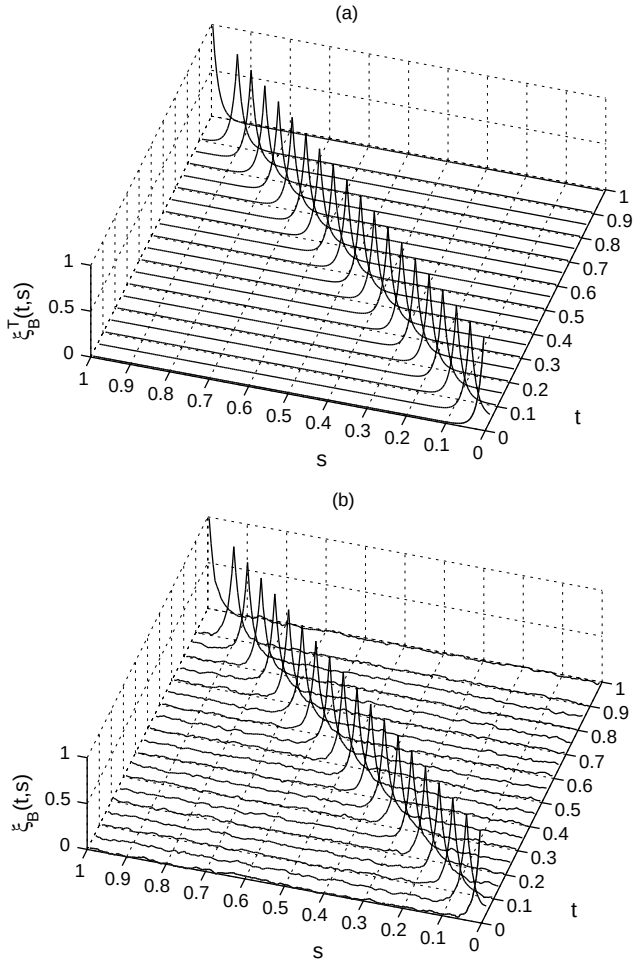

Fig. 13. Correlation distribution comparison for case B between (a) target and (b) ensemble of 10,000 samples of $\mathbf{Z}$ for ξ_B, where $\tau_0=0.03$.

approach that generates accurate underlying Gaussian input vectors.

Stochastic simulation of statistically inhomogeneous media is also investigated as a field of potential interest

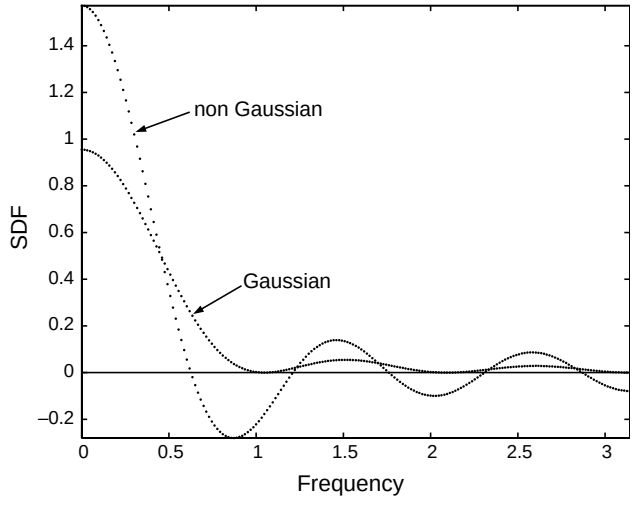

Fig. 14. Spectral density functions (SDFs) corresponding to ξ_{A} and $\xi_{\mathrm{g,A}}$.

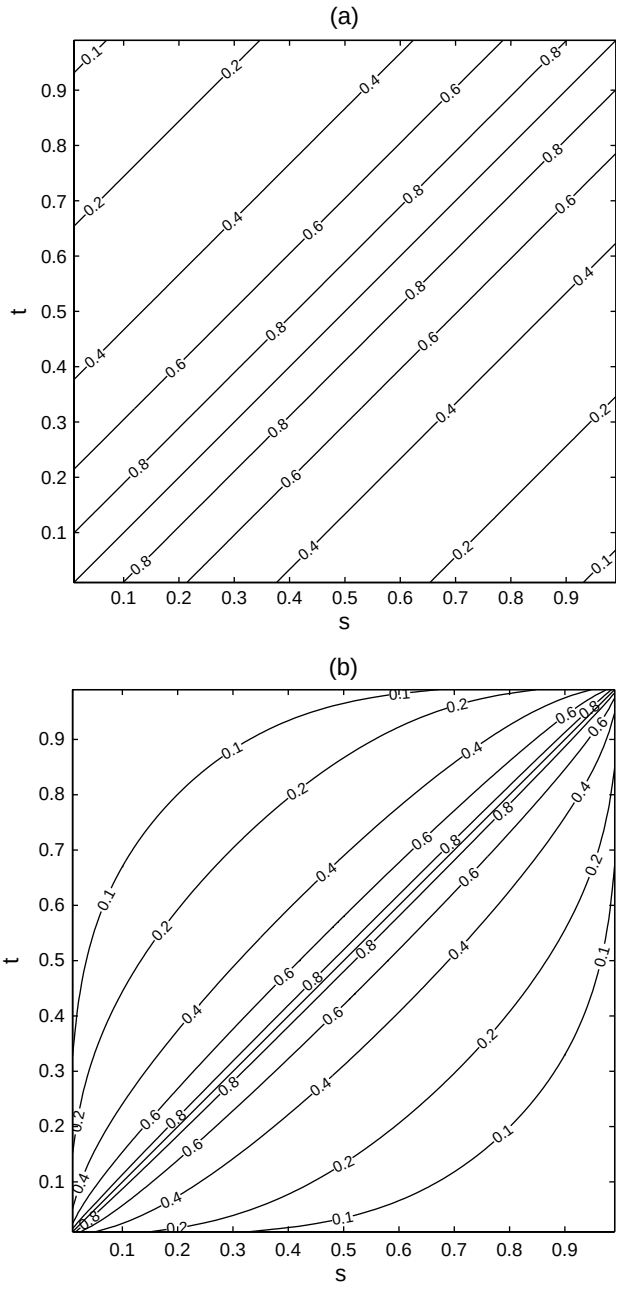

Fig. 15. Contour lines for (a) target Gaussian correlation $\xi_{g,\mathrm{A}}^T(t,s)$ and (b) its corresponding target non-Gaussian correlation $\xi_{\mathrm{A}}^T(t,s)$ with $\tau_0=0.4$.

for such processes. The non-stationarity present in the first order moments, which in this case is directly connected to the volume fraction content of the material, must be clearly considered by the simulating scheme. A binary translation based on non-stationary level-cuts of Gaussian processes is presented. The correlation distortion analysis for this case indicates that, while the limiting bounds developed by the theory must be observed, these are also consistent with the physical constraints of the problem. Resulting samples match the extreme non-Gaussian nature of the temporally dependent bimodal marginal pdfs, as well as the target second moment order properties.

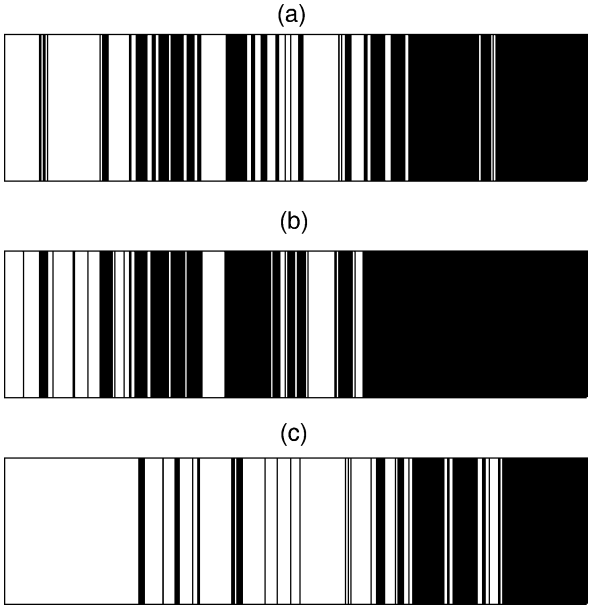

Fig. 16. Samples of Z with an exponential target Gaussian correlation $\xi^T_{g,A}(t,s)$ with $\tau_0=0.05$ and (a) $m=1$, (b) 2 and (c) 0.5.

References

[1] Priestley MB. Evolutionary spectra and non-stationary processes. J R Stat Soc 1965;27:204–37.
[2] Shinozuka M, Jan C-M. Digital simulation of random processes and its applications. J Sound Vib 1972;25(1):111–28.
[3] Deodatis G. Non-stationary stochastic vector processes: seismic ground motion applications. Probabilist Eng Mech 1996;11:149–68.
[4] Li Y, Kareem A. Simulation of multivariate nonstationary random processes by FFT. J Eng Mech 1991;117(5):1037–58.
[5] Gurley K, Kareem A. Applications of wavelet transforms in earthquake, wind and ocean engineering. Eng Struct 1999;21:149–67.
[6] Grigoriu M. Parametric models of nonstationary Gaussian processes. Probabilist Eng Mech 1995;10:95–102.
[7] Yamazaki F, Shinozuka M. Digital simulation of non-Gaussian stochastic fields. J Eng Mech 1988;114(6):1183–97.
[8] Deodatis G, Micaletti R. Simulation of highly skewed non-Gaussian stochastic processes. J Eng Mech 2001;127(12):1284–95.
[9] Masters F, Gurley K. Non-Gaussian simulation: cumulative distribution function map-based spectral correction. J Eng Mech 2003; 129(12):1418–28.
[10] Grigoriu M. Simulation of stationary non-Gaussian translation processes. J Eng Mech 1998;124(2):121–6.
[11] Ghanem R, Spanos P. Stochastic finite elements: a spectral approach. New York: Springer; 1991.
[12] Grigoriu M, Divletsen O, Arwade SR. A Monte Carlo simulation model for stationary non-Gaussian processes. Probabilist Eng Mech 2003;18:87–95.
[13] Arwade SR. Translation vectors with non-identically distributed components. Probabilist Eng Mech; 2005;20(2):158–67.
[14] Sakamoto S, Ghanem R. Simulation of multi-dimensional non-Gaussian non-stationary random fields. Probabilist Eng Mech 2002; 17:167–76.
[15] Phoon KK, Huang SP, Quek ST. Simulation of second-order processes using Karhunen-Loeve expansion. Comput Struct 2002; 80:1049–60.
[16] Ferrante F, Graham-Brady LL. Stochastic simulation of non-Gaussian, non-stationary properties in a functionally graded plate. Comput Methods Appl Mech Eng 2005;194:1675–92.
[17] Koutsourelakis S, Deodatis G. Simulation of binary random fields with applications to two-phase random media. J Eng Mech 2005; 131(4):397–412.
[18] Grigoriu M. Random field models for two-phase microstructures. J Appl Phys 2003;94(6):3762–70.
[19] Roberts AP, Knackstedt MA. Structure-property correlations in model composite materials. Phys Rev E 1996;54(3):2313–38.
[20] Yeong CLY, Torquato S. Reconstructing random media. Phys Rev E 1998;57(1):495–506.
[21] Quintanilla J, Torquato S. Microstructure functions for a model of statistically inhomogeneous random media. Phys Rev E 1997;55(2): 1558–65.
[22] Arwade SR, Grigoriu M. A model for non-stationary and anisotropic polycrystalline microstructures Ninth international conference on applications of statistics and probability in civil engineering, San Francisco, USA, July 6–9 2003.
[23] Arwade SR, Grigoriu M. Probabilistic model for polycrystalline microstructures with application to intergranular fracture. J Eng Mech 2004;130(9):997–1005.
[24] Grigoriu M. Applied non-Gaussian processes: examples, theory, simulation, random vibrations and MATLAB solutions. Englewood Cliffs, NJ: Prentice-Hall; 1995.
[25] Yamazaki F, Shinozuka M. Simulation of stochastic fields by statistical preconditioning. J Eng Mech 1990;116(2):268–87.
[26] Grigoriu M, Balopoulou S. Simulation method for stationary gaussian random functions based on sampling theorem. Probabilist Eng Mech 1993;8:239–54.
[27] Hotelling H, Pabst MR. Rank correlation and tests of significance involving no assumption of normality. Ann Math Stat 1936;7(1): 29–43.
[28] Phoon KK, Quek ST, Huang H. Simulation of non-Gaussian processes using fractile correlation. Probabilist Eng Mech 2004;19(4):287–92.
[29] Liu P-L, Kiureghian AD. Multivariate distribution models with prescribed marginals and covariances. Probabilist Eng Mech 1986; 1(2):105–12.
[30] Aboudi J, Pindera M, Arnold A. Thermoelastic theory for the response of materials functionally graded in two directions. Int J Solids Struct 1996;33(7):931–66.
[31] Suresh S, Mortensen A. Fundamentals of functionally graded materials. Cambridge: IOM Communications Ltd; 1998.
[32] Nadeau JC, Ferrari M. Microstructural optimization of a functionally graded transversely isotropic layer. Mech Mater 1999;31:637–51.
[33] Buryachenko V, Rammerstorfer F. Local effective thermoelastic properties of graded random structure matrix composites. Arch Appl Mech 2001;71(4–5):249–72.